Superluminal X-shaped beams propagating without distortion along a coaxial guide

Michel Zamboni-Rached* and K. Z. Nóbrega
DMO-FEEC, State University at Campinas, Campinas, SP, Brazil

Erasmo Recami†
Facoltà di Ingegneria, Università statale di Bergamo, Dalmine (BG), Italy;
INFN, Sezione di Milano, Milan, Italy

Hugo Enrique Hernández-Figueroa
DMO–FEEC, State University at Campinas, Campinas, SP, Brazil

In a previous paper we showed that localized superluminal solutions to the Maxwell equations exist, which propagate down (nonevanescence) regions of a metallic cylindrical waveguide. In this paper we construct analogous nondispersive waves propagating along coaxial cables. Such new solutions, in general, consist in trains of (undistorted) superluminal "X-shaped" pulses. Particular attention is paid to the construction of *finite* total energy solutions. Any results of this kind may find application in the other fields in which an essential role is played by a wave equation (like acoustics, geophysics, etc.).

I. INTRODUCTION

In a previous paper [1] we constructed localized superluminal solutions to the Maxwell equations propagating along (nonevanescent regions of) a metallic cylindrical waveguide. In the present paper we are going to show that analogous solutions exist even for metallic *coaxial* cables. Their interest is due to the fact that they propagate without distortion with superluminal group velocity.

Let us recall that already in 1915 Bateman [2] showed Maxwell equations to admit (besides of the ordinary solutions, endowed with speed c in vacuum) of wavelettype solutions, endowed in vacuum with group velocities $0 \leq v \leq c$. But Bateman's work went practically unnoticed, with the exception of a few authors as Barut *et al.* [3]. (Incidentally, Barut *et al.* even constructed a wavelettype solution [4] traveling with superluminal group velocity $V > c$.)

In recent times, however, many authors started to discuss the circumstance that all wave equations admit of solutions with $0 \leq v \leq \infty$: see, e.g., Ref. [5]. Most of those authors confined themselves to investigate (subluminal or superluminal) nondispersive solutions propagating in the open space only, namely, those solutions that had been called "undistorted progressive waves" by Courant and Hilbert [6].

Among localized solutions, the most interesting appeared to be the "X-*shaped waves*," which, predicted long ago to exist within special relativity in its extended version [7,8], had been mathematically constructed by Lu and Greenleaf [9] for acoustic waves, and by Ziolkowski *et al.* [10] and by Recami *et al.* [11] for electromagnetic waves.

Let us stress that such "X-shaped" localized solutions are superluminal (i.e., travel with a speed larger than c in vacuum) in the electromagnetic case; and are "supersonic"

(i.e., travel with a speed larger than the sound speed in the medium) in the acoustic case. The first authors to produce *experimentally* X-shaped waves were Lu and Greenleaf [13] for acoustics, Saari and Reivelt [14] for optics, and Mugnai *et al.* [15] for microwaves. Let us also emphasize, incidentally, that all such solutions can have an interesting role even in seismology, and probably in the gravitational wave sector.

Notwithstanding all that work [16], it is not well understood yet what solutions—let us now confine ourselves, for simplicity, to Maxwell equations and to electromagnetic waves only—have to enter into the play in realistic experiments using waveguides, optical fibers, etc.

II. THE CASE OF A CYLINDRICAL WAVEGUIDE

As we already mentioned, in Ref. [1] we constructed, for the TM (transverse magnetic) case, localized solutions to the Maxwell equations which propagate (undistorted) with Superluminal speed along a cylindrical waveguide. Let us take advantage of the present opportunity for calling further attention to two points, which received just a mention in Ref. [1], with regard to Eq. (9) and Fig. 2 therein. Namely, let us here stress that: (i) Those solutions consist in a *train* of pulses like the one depicted in Fig. 2 of Ref. [1]; and that (ii) each of such pulses is X-*shaped*.

A more complete representation of the TM [and transverse electric, TE] nondispersive waves, traveling down a cylindrical waveguide, will be forwarded elsewhere.

III. THE CASE OF A COAXIAL CABLE

Let us now examine the case of a coaxial cable (a metallic coaxial waveguide, to fix our ideas), that is, of the region delimited by two cylinders with radius $\rho = r_1$ and $\rho = r_2$, respectively, and axially symmetric with respect to the z axis: see Fig. 1. We shall consider in this article both the TM case,

---

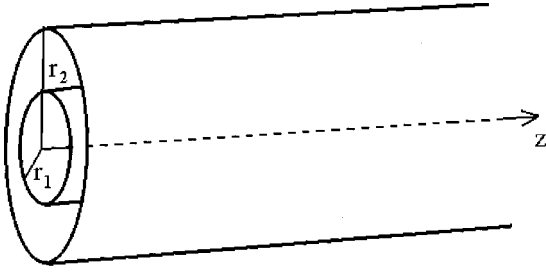*Email address: giz.r@uol.com.br
†Email address: recami@mi.infn.it

FIG. 1. Sketch of the coaxial waveguide.

characterized by the Dirichlet boundary conditions [17] (for any time instant t)

$$E_z(\rho=r_1;t)=0, \quad E_z(\rho=r_2;t)=0, \quad (1)$$

and the TE (transverse electric) case, characterized by the Neumann boundary conditions [17] (for any t),

$$\frac{\partial}{\partial\rho}H_z(\rho=r_1;t)=0, \quad \frac{\partial}{\partial\rho}H_z(\rho=r_2;t)=0. \quad (2)$$

To such aims, we shall first generalize a theorem due to Lu *et al.* [18] (stated and demonstrated below, in the Appendix), which showed how to start from a solution holding *in the plane* (x,y) for constructing a three-dimensional solution rigidly moving along the z axis with superluminal speed V. The theorem of Lu *et al.* was valid for the vacuum. In Ref. [1], we set forth its generalization for a cylindrical waveguide, while here we are going to extend it, as we said above, for a coaxial cable. Let us first recall what the theorem of Lu *et al.* is about. If we assume that $\psi(\boldsymbol{\rho};t)$, with $\boldsymbol{\rho}\equiv(x,y)$, is a solution of the two-dimensional homogeneous wave equation

$$\left(\partial_x^2+\partial_y^2-\frac{1}{c^2}\partial_t^2\right)\psi(\boldsymbol{\rho};t)=0, \quad (3)$$

then, by applying the transformations

$$\boldsymbol{\rho}\rightarrow\boldsymbol{\rho}\sin\theta, \quad \text{and} \quad t\rightarrow t-z\left(\frac{\cos\theta}{c}\right), \quad (4)$$

the angle θ being fixed, with $0<\theta<\pi/2$, one gets [18] that $\psi(\boldsymbol{\rho}\sin\theta;t-z\cos\theta/c)$ is now a solution of the *three-dimensional* homogeneous wave equation

$$\left(\nabla^2-\frac{1}{c^2}\partial_t^2\right)\psi\left(\boldsymbol{\rho}\sin\theta;t-z\frac{\cos\theta}{c}\right)=0, \quad (5)$$

where now $\nabla^2\equiv\partial_x^2+\partial_y^2+\partial_z^2$, $\boldsymbol{\rho}\equiv(x,y)$.

The mentioned theorem holds for the free case, so that, in general, it does not hold when introducing boundary conditions. We shall see, however, that it can be extended even to the case of a two-dimensional solution ψ valid on an annular domain, $a\leq\rho\leq b$, $\rho\equiv|\boldsymbol{\rho}|$, with either the (Dirichlet) boundary conditions

$$\psi(\rho=a;t)=\psi(\rho=b;t)=0, \quad (1')$$

or the (Neumann) boundary conditions

$$\frac{\partial}{\partial\rho}\psi(\rho=a;t)=\frac{\partial}{\partial\rho}\psi(\rho=b;t)=0. \quad (2')$$

Let us notice right now that transformations (4), with condition $(1')$ or $(2')$, lead to a (three-dimensional) solution rigidly traveling with superluminal speed $V=c/\cos\theta$ inside a coaxial cable with internal and external radius equal (no longer to a, b, but) to $r_1=a/\sin\theta>a$ and $r_2=b/\sin\theta>b$, respectively. The same procedure can be applied also in other cases, provided that the boundary conditions depend on x,y only, as in the case, e.g., of a cable with many cylindrical (empty) tunnels inside it.

IV. THE TRANSVERSE MAGNETIC (TM) CASE

Let us go back to the two-dimensional equation (3) with the boundary conditions $(1')$. Let us choose, for instance, the simple *initial* conditions $\psi(\rho;t=0)\equiv\phi(\rho)$ and $\partial\psi/\partial t\equiv\xi(\rho)$ at $t=0$, where

$$\phi(\rho)=\delta(\rho-\rho_0), \quad \xi(\rho)|_{t=0}=0, \quad (6)$$

with

$$a<\rho_0<b. \quad (6')$$

Following a method similar to that in Ref. [1], and using the boundary conditions $(1')$, in cylindrical coordinates and for axial symmetry one gets solutions to Eq. (3) of the type $\psi=\Sigma R_n(\rho)T_n(t)$ in the following form:

$$2\psi(\rho;t)=\sum_{n=1}^{\infty}R_n(\rho)[A_n\cos\omega_n t-B_n\sin\omega_n t], \quad (7)$$

where the functions $R(\rho)$ are

$$R_n(\rho)\equiv N_0(k_n a)\ J_0(k_n\rho)-J_0(k_n a)\ N_0(k_n\rho), \quad (8)$$

quantities N_0 and J_0 being the zeroth-order Neumann and Bessel functions, respectively; and where the characteristic angular frequencies [19] can be evaluated numerically, they being solutions to the equation $[\omega_n=ck_n]$,

$$\frac{J_0(k_n a)}{N_0(k_n a)}=\frac{J_0(k_n b)}{N_0(k_n b)}. \quad (9)$$

The initial conditions (6) imply that $\Sigma A_n R_n(\rho)=\delta(\rho-\rho_0)$, and $\Sigma B_n R_n(\rho)=0$, so that all the coefficients B_n vanish, and eventually one obtains the two-dimensional solution

$$\Psi_{2D}(\rho;t)=\sum_{n=1}^{\infty}A_n R_n(\rho)\cos\omega_n t, \quad (10)$$

with

$$2A_n=\{-a^2[N_0(k_n a)J_1(k_n a)-J_0(k_n a)N_1(k_n a)]^2$$
$$+b^2[N_0(k_n a)J_1(k_n b)-J_0(k_n a)N_1(k_n b)]^2\}^{-1}$$
$$\times R_n(\rho_0). \quad (11)$$
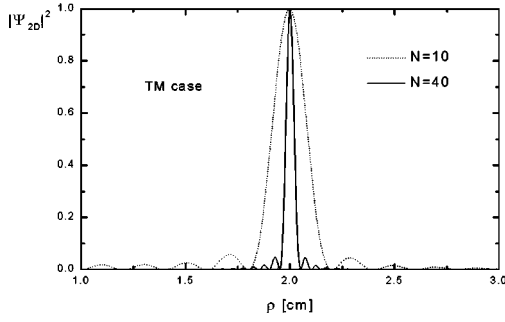
FIG. 2. Square magnitude $|\Psi_{2D}(\rho;t=0)|^2$ of the two-dimensional solutions in Eq. (10) for fixed time ($t=0$) and for $N=10$ (dotted line) or $N=40$ (solid line). It refers to the TM case (Dirichlet boundary conditions) with $a=1$ cm, $b=3$ cm, and $\rho_0=2$ cm: see the text.

One can notice that the present procedure is mathematically analogous to the analysis of the free vibrations of a ring-shaped elastic membrane [19].

For any practical purpose, one has of course to take a finite number N of terms in expansion (10). In Fig. 2 we show, e.g., the two-dimensional functions $|\Psi_{2D}(\rho;t)|^2$ of Eq. (10) for fixed time ($t=0$) and for $N=10$ (dotted line) or $N=40$ (solid line). Notice that, when the value N is finite, the first one of the conditions (6) is no longer a δ function, but represents a physical wave, which nevertheless is still clearly bumped (Fig. 2). It is rather interesting that, for each value of N, one meets a different (physical) situation; at the extent that we obtain infinite many *different* families of three-dimensional solutions, by varying the truncating value N in Eq. (12) below.

Actually, by the transformations (4) we arrive from Eq. (10) at the three-dimensional superluminal nondispersive solution Ψ_{3D}, propagating without distortion along a metallic coaxial waveguide, i.e., down a coaxial cable [$V>c$],

$$\Psi_{3D}(\rho;z-Vt)=\sum_{n=1}^{\infty} A_n R_n(\rho \sin \theta) \cos[k_n(z-Vt)\cos \theta],$$
$$(12)$$

which is a sum over different propagating modes. The fact that $V=c/\cos \theta>c$ means (once more) that the group velocity[1] of our pulses is superluminal. For simplicity, in our figures we shall put $z-Vt\equiv\eta$.

Let us notice that transformations (4), which change—as we already know—a into $r_1=a/\sin \theta$ and b into $r_2=b/\sin \theta$, are such that the maximum of Ψ_{3D} is got for the

_____

[1]Let us recall that the group-velocity is well defined only when the pulse has a clear bump in space; but it can be calculated by the approximate relation $v_g\simeq d\omega/d\beta$, quantity β being the wave number, *only* when some extra conditions are satisfied (namely, when ω as a function of β is also clearly bumped). In the present case the group velocity is very well defined, but cannot be evaluated through that simple relation, since ω is a discrete function of β; cf. Eq. (9) and Sec. VI, Eq. (22), below.

value $\rho_0/\sin \theta$ of ρ. However, solution (12) does automatically satisfy on the cylinders with radius r_1 and r_2 the conditions [$\Psi_{3D}\equiv E_z$],

$$\Psi_{3D}(\rho=a/\sin \theta,z;t)=\Psi_{3D}(\rho=b/\sin \theta,z;t)=0.$$

Till now, Ψ_{3D} has represented the electric field component E_z. Let us add that in the TM case [20]

$$\boldsymbol{E}_{\perp}=i\frac{cV}{V^2-c^2}\sum_{n=1}^{\infty}\frac{1}{k_n}\boldsymbol{\nabla}_{\perp}\Psi_{3D}, \qquad (12\text{a})$$

where

$$\frac{cV}{V^2-c^2}\equiv\frac{\cos \theta}{\sin^2\theta}, \quad k_n=\omega_n/c,$$

and

$$\boldsymbol{H}_{\perp}=\varepsilon_0\frac{V}{c}\ \hat{\boldsymbol{z}}\times\boldsymbol{E}_{\perp}. \qquad (12\text{b})$$

As we mentioned above, for any truncating value N in expansion (10), we get a *different* physical situation: In a sense, we excite in a *different* way the two-dimensional annular membrane, obtaining (via the theorem of Lu) different three-dimensional solutions, which correspond [1] to nothing but summation (12) truncated at the value N.

In Figs. 3(a), 3(b), we show a single (X-shaped) three-dimensional pulse Ψ_{3D} with $\theta=84^{\circ}$, and $N=10$ or $N=40$, respectively.

In Fig. 4, by contrast, we depict a couple of elements of the *train* of X-shaped pulses represented by Eq. (12), for $\theta=45^{\circ}$ and $N=40$.

In Fig. 5 the orthogonal projection is moreover shown of a single pulse (of the solution in Fig. 4) onto the (ρ,z) plane for $t=0$, with $\theta=45^{\circ}$ and $N=40$. Quantities ρ and η are always in centimeters.

V. THE TRANSVERSE ELECTRIC (TE) CASE

In the TE case, one has to consider the two-dimensional equation (3) with the boundary conditions (2′), while the initial conditions (6) can remain the same.

As in Sec. IV, one gets—still for axial symmetry in cylindrical coordinates—the following solution to Eq. (3):
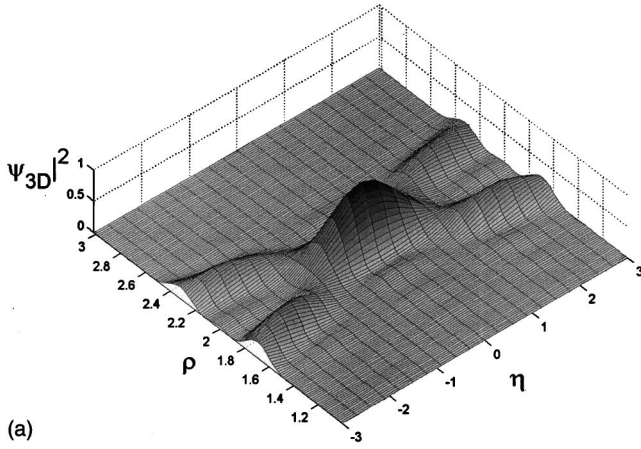
$$2\psi(\rho;t)=\sum_{n=1}^{\infty} R_n(\rho)[A_n \cos \omega_n t-B_n \sin \omega_n t], \quad (13)$$
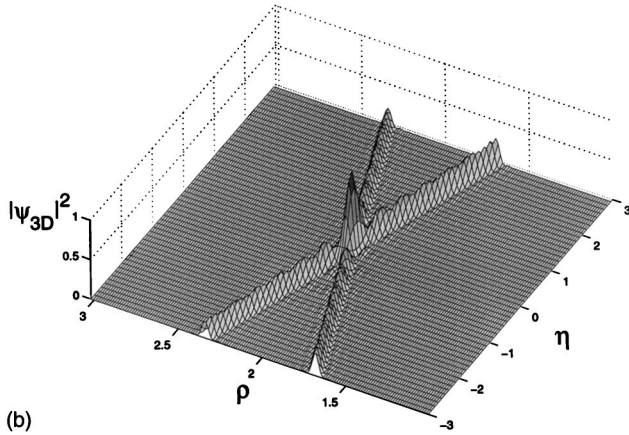
where now the functions $R_n(\rho)$ are

$$R_n(\rho)\equiv N_1(k_n a)J_0(k_n\rho)-J_1(k_n a)N_0(k_n\rho), \quad (13')$$

defined in terms of different values of k_n. In fact, the characteristic (angular) frequencies are now to be obtained by the new relation

$$\frac{J_1(k_n a)}{N_1(k_n a)}=\frac{J_1(k_n b)}{N_1(k_n b)}. \qquad (14)$$

(a)

(b)

FIG. 3. In Figs. (a) and (b) we show the square magnitude $|\Psi_{3D}(\rho,\eta)|^2$ of a single (X-shaped) three-dimensional pulse of the beam in Eq. (12), with $\theta=84^\circ$, $r_1=a/\sin\theta$, $r_2=b/\sin\theta$ (it having been chosen $a=1$ cm and $b=3$ cm), for $N=10$ and $N=40$, respectively. They refer to the TM case. Notice that $\eta\equiv z-Vt$, and that the considered beam is a train of X-shaped pulses. In all the figures of this paper, quantities ρ and η are in centimeters.

Again, the initial conditions (6) entail that $\Sigma A_n R_n(\rho) = \delta(\rho-\rho_0)$, and $\Sigma B_n R_n(\rho)=0$, so that all the coefficients B_n vanish, and one gets the two-dimensional solution

$$\Psi_{2D}(\rho;t)=\sum_{n=1}^{\infty} A_n R_n(\rho)\cos\omega_n t, \qquad (15)$$

where the coefficients A_n are given by

$$2A_n=\{-a^2[N_1(k_n a)J_0(k_n a)-J_1(k_n a)N_0(k_n a)]^2$$
$$+b^2[N_1(k_n a)J_0(k_n b)-J_1(k_n a)N_0(k_n b)]^2\}^{-1}$$
$$\times R_n(\rho_0). \qquad (15')$$

In this case one obtains, by transformations (4), the superluminal nondispersive three-dimensional solution

$$\Psi_{3D}(\rho;z-Vt)=\sum_{n=1}^{\infty} A_n R_n(\rho\sin\theta)\cos[k_n(z-Vt)\cos\theta],$$
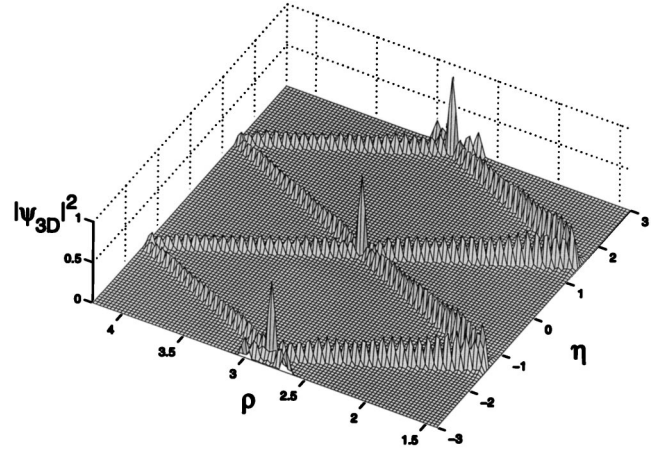$$(16)$$

FIG. 4. In this figure we depict, by contrast, a *couple* of elements of the train of X-shaped pulses represented in the TM case by Eq. (12), for $N=40$. This time the angle $\theta=45^\circ$ was chosen, keeping the same a and b values as before.

propagating along the metallic coaxial waveguide with group velocity $V=c/\cos\theta>c$. The present solution (16) satisfies the boundary conditions

$$\frac{\partial}{\partial\rho}\Psi_{3D}(\rho,z;t)\bigg|_{\rho=a/\sin\theta}=\frac{\partial}{\partial\rho}\Psi_{3D}(\rho,z;t)\bigg|_{\rho=b/\sin\theta}=0,$$

where now $\Psi_{3D}\equiv H_z$. The transverse components, in the TE case, are given [20] by

$$\boldsymbol{H}_\perp=\frac{-cV}{V^2-c^2}\sum_{n=1}^{\infty}\frac{1}{k_n}\sin[k_n(z-Vt)\cos\theta]\boldsymbol{\nabla}_\perp R_n(\rho\sin\theta),$$
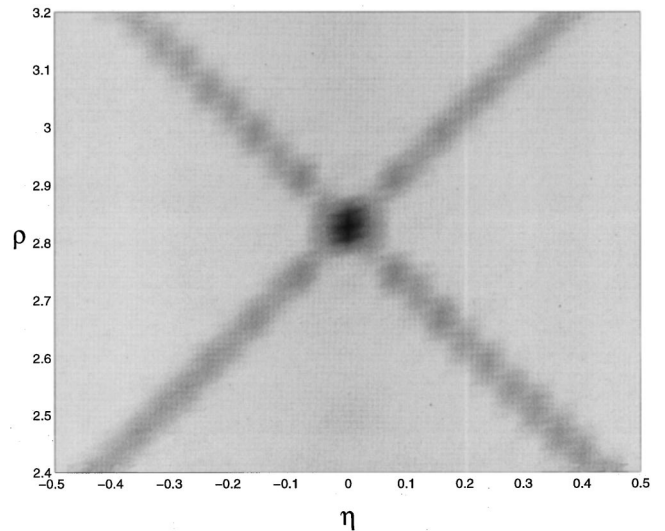$$(17a)$$

and

FIG. 5. The orthogonal projection is shown of a single pulse (of the solution in Fig. 4, referring to the TM case) onto the (ρ,z) plane for $t=0$, with $\theta=45^\circ$ and $N=40$.
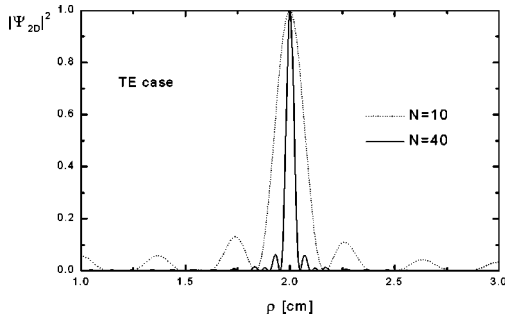
FIG. 6. In analogy with Fig. 2, the square magnitude $|\Psi_{2D}(\rho;t=0)|^2$ is shown of the two-dimensional solutions in Eq. (15) for fixed time ($t=0$), and for $a=1$ cm, $b=3$ cm, $\rho_0=2$ cm; this time it refers, however, to the TE case (Neumann boundary conditions); see the text. Again, the dotted line corresponds to $N=10$, and the solid line to $N=40$.

$$\boldsymbol{E}_\perp = -\mu_0 \frac{V}{c}\,\hat{z}\times\boldsymbol{H}_\perp\,. \tag{17b}$$

In Fig. 6 we plot our function Ψ_{2D} with $N=10$ (dotted line) or $N=40$ (solid line). In Fig. 7 there are depicted, by contrast, two elements of the train of X-shaped pulses represented by Eq. (16), with $\theta=60^\circ$, for $N=40$ only. In Fig. 8, at last, we show the orthogonal projection of the solution in Fig. 7 onto the plane (ρ,z) for $t=0$, with $\theta=60^\circ$ and $N=40$. Quantities ρ and η are in cm.

VI. REDERIVATION OF OUR RESULTS FROM THE STANDARD THEORY OF WAVEGUIDE PROPAGATION

Lu's theorem is certainly a very useful tool to build up localized solutions to Maxwell equations: nevertheless, due to the novelty of our previous results, it may be worthwhile to outline an alternative derivation [1] of them which can sound more familiar. To such an aim, we shall follow the procedure introduced in Ref. [1].

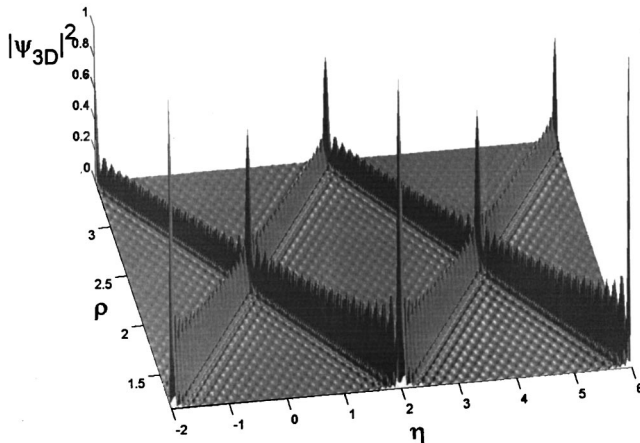For the sake of simplicity, let us limit ourselves to the

FIG. 7. In this figure, which refers to the TE case, two elements are depicted of the train of X-shaped pulses represented by Eq. (16), with $\theta=60^\circ$ and $N=40$, while keeping the same a and b values as before.
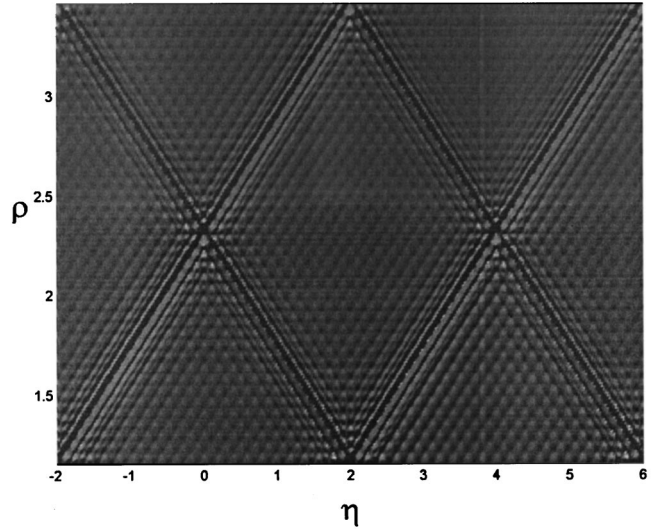

FIG. 8. The orthogonal projection is shown of the solution in Fig. 7, for the TE case, onto the plane (ρ,z) for $t=0$, with $\theta=60^\circ$ and $N=40$.

domain of TM modes. When a solution in terms of the longitudinal electric component E_z is sought, one has to deal with the boundary condition $E_z=0$; we shall look, moreover, for axially symmetric solutions (i.e., independent of the azimuth variable φ): Such choices could be easily generalized, just at the cost of increasing the mathematical complexity. Quantity E_z is then completely equivalent to the scalar variable $\Psi\equiv\Psi_{3D}$ used in the previous analysis.

Let us look for solutions of the form [1]

$$E_z(\rho,z;t)=KR(\rho)\exp\left[i\left(\frac{\omega z\cos\theta}{c}-\omega t\right)\right], \tag{18}$$

where $R(\rho)$ is assumed to be a function of the radial coordinate ρ only, and K is a normalization constant. Here we call c the velocity of light in the medium filling the coaxial waveguide, supposing it nondispersive. The (angular) frequency ω is for the moment arbitrary.

By inserting expression (18) into the Maxwell equation for E_z, one obtains [1]

$$\rho^2\frac{\mathrm{d}^2R(\rho)}{\mathrm{d}\rho^2}+\rho\frac{\mathrm{d}R(\rho)}{\mathrm{d}\rho}+\rho^2\Omega^2R(\rho)=0,\quad \Omega\equiv\frac{\omega\sin\theta}{c},$$

whose only solution, which is finite on the waveguide axis, is $R(\rho)=N_0(\omega a/c)J_0(\omega\rho\sin\theta/c)-J_0(\omega a/c)N_0(\omega\rho\sin\theta/c)$, which is analogous to Eq. (8).

By imposing the boundary conditions $R(\rho)=0$ for $\rho=r_1$ and $\rho=r_2$, one gets the acceptable frequencies from the characteristic equation,

$$\frac{J_0(\omega_n a/c)}{N_0(\omega_n a/c)}=\frac{J_0(\omega_n b/c)}{N_0(\omega_n b/c)}, \tag{19}$$

so that one has a different function $R_n(\rho)$ for each value of ω_n. Therefore, assuming [1] an arbitrary parameter θ, we find that, for every mode supported by the waveguide and

labeled by the index n, there is just one frequency at which the assumed dependence (18) on z and t is physically realizable. Let us show such a solution to be the standard one known from classical electrodynamics. In fact, by inserting [1] the allowed frequencies ω_n into the complete expression of the mode, we have

$$E_z^n(\rho,z;t) = KR_n(\rho) \exp\left[i\left(\frac{\omega_n z \cos\theta}{c} - \omega_n t\right)\right]. \quad (20)$$

But the generic solution for (axially symmetric) TM$_{0n}$ modes [21] in a coaxial metallic waveguide is [$\Omega_n \equiv \omega_n \sin\theta/c$],

$$E_z^{\mathrm{TM}_{0n}} = KR_n(\rho) \exp[i(\beta(\omega_n)z - \omega_n t)], \quad (21)$$

the wave number β being a discrete function of ω, with the "dispersion relations"

$$\beta^2(\omega_n) = \frac{\omega_n^2}{c^2} - \Omega_n^2.$$

By identifying $\beta(\omega_n) \equiv \omega_n \cos\theta/c$, as suggested by Eq. (20), and remembering the expression for ω_n given by Eq. (19), the ordinary dispersion relation is got [1]. We have therefore verified that every term in the expansion (12) is a solution to Maxwell equations not different from the usual one.

The uncommon feature of our solution (12) is that, given a particular value of θ, the phase velocity of *all* its terms is always the same, it being independent of the mode index n,

$$V_{\mathrm{ph}} = \left[\frac{\beta(\omega_n)}{\omega_n}\right]^{-1} = \frac{c}{\cos\theta}.$$

In such a case it is well known that the group velocity of the pulse *equals* the phase velocity [22]: and in our case is the velocity *tout court* of the localized pulse.

With reference to Fig. 9, we can easily see [1] that all the allowed values of ω_n can be calculated by determining the intersections of the various branches of the dispersion relation with a straight line, whose slope depends on θ only. By using suitable combinations of terms, corresponding to different indices n, as in our Eq. (12), it is possible to describe a disturbance having a time-varying profile [1], as already shown in Figs. 3–4 above. Each pulse thus displaces itself *rigidly*, with a *velocity* $v \equiv v_g$ equal to V_{ph}.

It should be repeated that the velocity v (or group-velocity $v_g \equiv v$) of the pulses corresponding to Eq. (9) is not to be evaluated by the ordinary formula $v_g \simeq d\omega/d\beta$ (valid for quasimonochromatic signals). This is at variance with the common situation in optical and microwave communications, when the signal is usually an "envelope" superimposed to a carrier wave whose frequency is generally much higher than the signal bandwidth. In *that* case the standard formula for v_g yields the correct velocity to deal with (e.g., when propagation delays are studied). Our case, on the contrary, is much more reminiscent of a baseband modulated signal, as those studied in ultrasonics: the very concept of a carrier becomes meaningless here, as the discrete "harmonic" components have widely different frequencies [1].
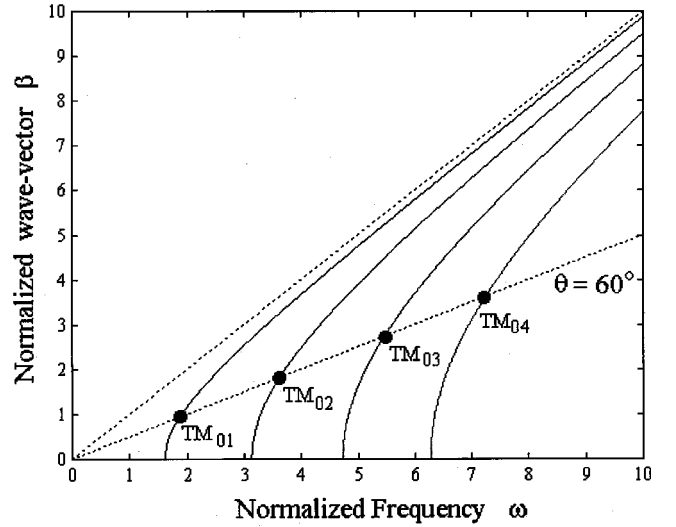

FIG. 9. Dispersion curves for the symmetrical TM$_{0n}$ modes in a perfect coaxial waveguide, and location of the frequencies whose corresponding modes possess the same phase velocity. [Actually, the phase velocity $c/\cos\theta$ of all the terms in expansion (12) is always the same, being independent of the mode index n: In such a case, it is known that the group velocity of the pulse (namely, the velocity *tout court* of the localized pulse) becomes equal to the phase velocity.]

Let us finally remark [1] that similar considerations could be extended to all the situations where a waveguide supports several modes. Tests at microwave frequencies should be rather easy to perform; by contrast, experiments in the optical domain would face the problem of the limited extension of the spectral windows corresponding to not too large attenuation, even if some work [23] is in progress in many directions.

Moreover, results of the kind presented in this paper, as well as in Refs. [1,11,12], may find application in the other fields in which an essential role is played by a wave equation (like acoustics, seismology, geophysics, and relativistic quantum mechanics, possibly).

VII. HOW TO GET FINITE TOTAL ENERGY SOLUTIONS

We shall go on following the standard formalism of Sec. VI; what we are going to do holds, however, for both the TM and the TE case. Let us anticipate that, in order to get finite total energy solutions (FTES), we shall have to replace each characteristic frequency ω_n [cf. Eq. (9), or Eq. (14), or rather Fig. 9] by a *small* frequency band $\Delta\omega$ centered at ω_n, always choosing the same $\Delta\omega$ independently of n. In fact, since all the modes entering the Fourier-type expansion (12), or (16), possess the same phase velocity $V_{\mathrm{ph}} \equiv V = c/\cos\theta$, each small bandwidth packet associated with ω_n will possess the same group velocity $v_g = c^2/V_{\mathrm{ph}}$, so that we shall have as a result a wave whose *envelope* travels with the *subluminal* group velocity v_g. *However*, inside the subluminal envelope, one or more *pulses* will be traveling with the dual (superluminal) speed $V = c^2/v_g$. Such well-localized peaks have nothing to do with the ordinary (sinusoidal) carrier wave,

and will be regarded as constituting *the relevant* wave. Before going on, let us mention that previous work related to FTESs can be found—as far as we know—only in Refs. [24,12].

Formally, to get FTESs, let us consider the ordinary (three-dimensional) solutions for a coaxial cable:

$$\psi_n(\rho,z;t) = K_n R_n(\rho) \cos[\beta(\omega)z - \omega t], \qquad (22)$$

where coefficients K_n *coincide* with the A_n given by Eq. (11) or Eq. (15') in the TM or TE cases, respectively; and functions R_n are again given by Eq. (8) or Eq. (13'), respectively; since the values k_n,

$$k_n \equiv \frac{\omega^2}{c^2} - \beta^2, \qquad (23)$$

are equal to those found via the (two dimensional) Eq. (9) in the TM and via Eq. (14) in the TE case, simply *multiplied* by $\sin\theta$ [because of the fact that, when going on from the two-dimensional membrane to the three-dimensional coaxial cable, the internal and external radia are equal (no longer to a, b, but) to $r_1 = a/\sin\theta$ and $r_2 = b/\sin\theta$].

Let us now consider the spectral functions

$$W_n \equiv \exp[-q^2(\omega - \omega_n)^2], \qquad (24)$$

with the same weight parameter q, so that $\Delta\omega$ too is the same [according to our definitions, $\Delta\omega = 1/q$]; and with

$$\omega_n \equiv \frac{k_n c}{\sin\theta}, \qquad (25)$$

quantity $\sin\theta$ having a fixed but otherwise arbitrary value. We shall construct FTESs, $\mathcal{F}(\rho,z;t)$, of the type[2]

$$\mathcal{F}_{3D}(\rho,z;t) = \sum_{n=1}^{N} \int_{-\infty}^{\infty} d\omega\, \psi_n W_n, \qquad (26)$$

with arbitrary N. Notice that we are not using a single Gaussian weight, but a different Gaussian function for each ω_n value, such weights being centered around the corresponding ω_n.

Due to the mentioned localization of the W_n around the ω_n values, we can (for each value of n in the above sum) expand the function $\beta(\omega)$ in the neighborhood of the corresponding ω_n value:

$$\beta(\omega) \simeq \beta_{0n} + \frac{\partial\beta}{\partial\omega}\bigg|_{\omega_n} (\omega - \omega_n) + \cdots, \qquad (27)$$

---

[2]When integrating over ω from $-\infty$ to $+\infty$ there are also the nonphysical (traveling backwards in space) and the evanescent waves. But their actual contribution is totally negligible, since the weight functions W_n are strongly localized in the vicinity of the ω_n values (which are all positive; see, e.g., Fig. 9). In any case, one could integrate from 0 to ∞ at the price of increasing a little the mathematical complexity: we are preferring the present formalism for the sake of simplicity.

where $\beta_{0n} = \omega_n \cos\theta$, and the further terms are neglected since $\Delta\omega$ is assumed to be small. Notice that, because of relations (25) and (23), in Eq. (27) the group velocities, given by

$$\frac{1}{v_{gn}} = \frac{\partial\beta}{\partial\omega}\bigg|_{\omega_n},$$

are actually independent of n, all of them possessing therefore the same value:

$$v_{gn} \equiv v_g = c\cos\theta. \qquad (27')$$

By using relation (27) and the transformation of variables

$$f_n \equiv \omega - \omega_n,$$

the integration in Eq. (26) does eventually yield

$$\mathcal{F}_{3D}(\rho,z;t) = \frac{\sqrt{\pi}}{q} \exp\left[-\frac{(z - v_g t)^2}{4q^2 v_g^2}\right] \sum_{n=1}^{\infty} A_n R_n(\rho)$$
$$\times \cos[k_n(z - Vt)\cos\theta], \qquad (28)$$

where, let us recall, $V = c^2/v_g = c/\cos\theta$, and we used the identity

$$\int_{-\infty}^{\infty} df \exp[-q^2 f^2] \cos[f(v_g^{-1}z - t)]$$
$$= \frac{\sqrt{\pi}}{q} \exp\left[-\frac{(v_g^{-1}z - t)^2}{4q^2}\right].$$

It is rather interesting to notice that the FTES (28) is related to the X-shaped waves, since the integration in Eq. (26) does eventually yield the FTES in the form

$$\mathcal{F}_{3D}(\rho,z;t) = \frac{\sqrt{\pi}}{q} \exp\left[-\frac{(z - v_g t)^2}{4q^2 v_g^2}\right] \mathcal{T}(\rho,z), \qquad (29)$$

function $\mathcal{T}(\rho,z)$ being one of our previous solutions in Eq. (12) or Eq. (16) above, at our free choice.

Let us go back to the important relation (27'), and to the discussion about it started at the beginning of this section. Let us repeat that, if we choose the ω_n values as in Fig. 9, all our small-bandwidth packets, centered at the ω_n's, get the same phase velocity $V > c$ and therefore the same group velocity $v_g < c$ [since for metallic waveguides the quantities $k_n^2 = \omega_n^2/c^2 - \beta^2$ are constant for each mode, and $v_g \equiv \partial\omega/\partial\beta$, so that it is $Vv_g = c^2$]. This means that the envelope of solution (28) and (29) moves with slower-than-light speed; the envelope length[3] Δl depending on the chosen $\Delta\omega$, and being therefore proportional to qv_g.

However, inside such an envelope, one gets a train of (X-shaped) pulses—having nothing to do with the ordinary

---

[3]One may call "envelope length" the distance between the two points in which the envelope height is, for instance, 10% of its maximum height.
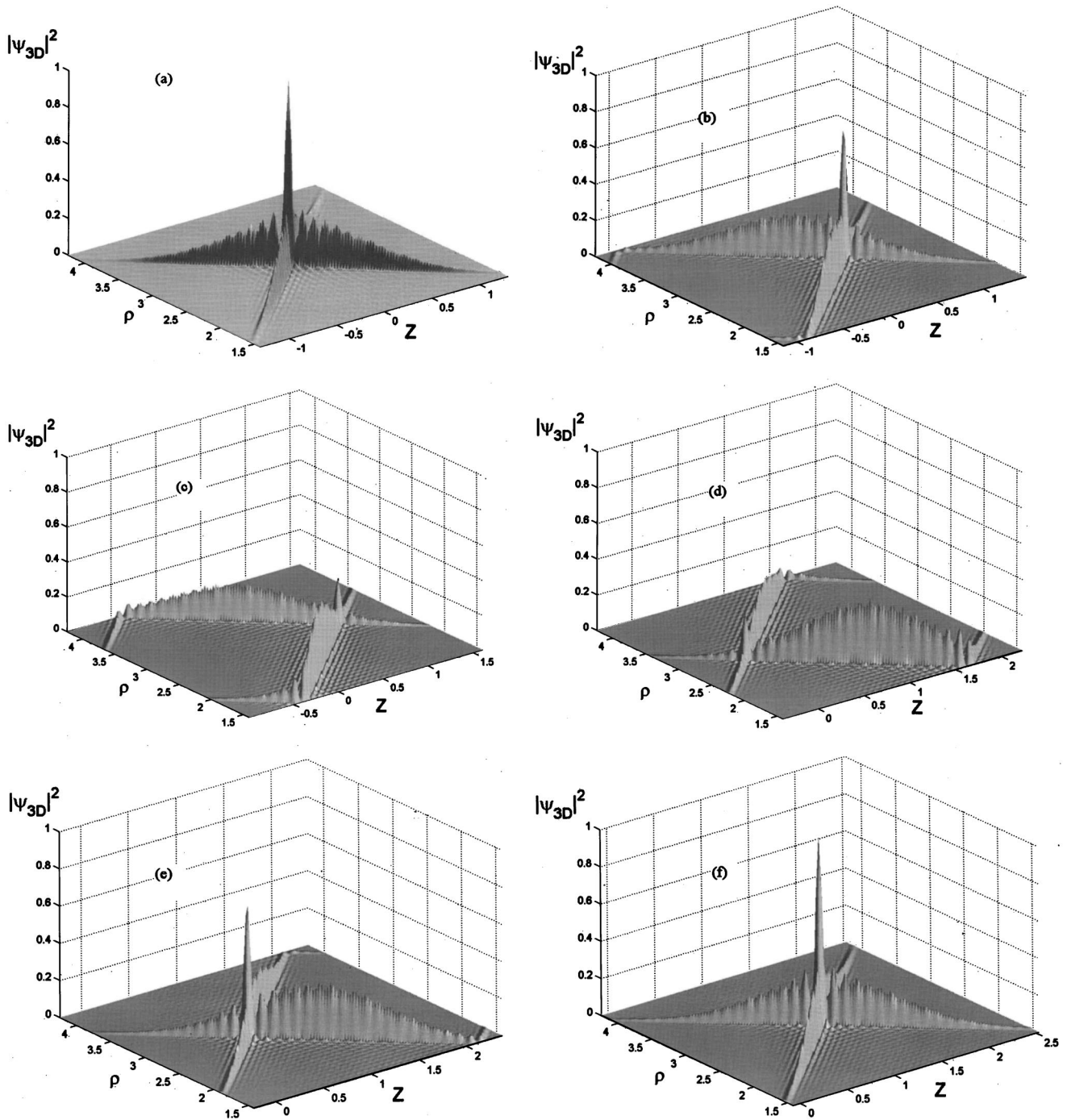
FIG. 10. Time evolution of a *finite* total energy solution. Choosing $q = 0.606$ s, $c = 1$, $N = 40$, $a = 1$ cm, $b = 3$ cm, and $\theta = 45°$, there is only *one* X-shape pulse inside the subluminal envelope: see the text. The pulse and envelope velocities are given by $V = 1/\cos\theta$ and $v_g = 1/V$: The superluminal speed $V = 1/v_g$ of such a pulse can be regarded, of course, as the actual velocity of the wave. Figures (a), (b), (c), (d), (e), and (f) show a complete cycle of the pulse; they correspond to the time instants $t = 0$, $t = 0.5$ s, $t = 1$ s, $t = 3$ s, $t = 3.5$ s, and $t = 4$ s, respectively.

carrier wave,[4] as we already mentioned—traveling with the superluminal speed V. An interesting point is that we can choose the envelope length so that it contains *only one* (X-

shaped wave) peak: the superluminal speed $V = c^2/v_g$ of such a pulse can then be regarded as the actual velocity of the wave. In order to have just one peak inside the envelope, the envelope length is to be chosen smaller than the distance between two successive peaks of the (infinite total energy) train (12), or (16).

---

[4]Actually, they can be regarded as a sum of carrier waves.

It should be noted, at last, that the amplitude of such a single X-shaped pulse (which remains confined inside the envelope) first increases, and afterwards decreases, while traveling; till when it practically disappears. While the considered pulse tends to vanish on the right (i.e., under the right tail of the envelope), a second pulse starts to be created on the left; and so on. From Eq. (29) it is clear, in fact, that our finite-energy solution is nothing but an (infinite-energy) solution of the type in Eq. (12), or in Eq. (16), multiplied by a Gaussian function. In Fig. 10 all such a behavior is clearly depicted.

APPENDIX

Let us here state, and demonstrate, the Lu's theorem, for the reader's convenience:

Theorem. Be $\psi_{2D}(x,y;t)$ a solution of the two-dimensional homogeneous wave equation

$$\left(\partial_x^2 + \partial_y^2 - \frac{1}{c^2} \partial_t^2 \right) \psi_{2D}(x,y;t) = 0. \quad (A1)$$

On applying the transformations

$$x \to x' \sin \theta, \quad y \to y' \sin \theta, \quad \text{and} \quad t \to t' - z' \frac{\cos \theta}{c}, \quad (A2)$$

the angle θ being fixed $(0 < \theta < \pi/2)$, the three-dimensional function

$$\psi_{3D}(x',y',z';t') = \psi_{2D}(x' \sin \theta, y' \sin \theta; t' - z' \cos \theta/c) \quad (A3)$$

results to be a solution of the three-dimensional wave equation

$$\left(\partial_{x'}^2 + \partial_{y'}^2 + \partial_{z'}^2 - \frac{1}{c^2} \partial_{t'}^2 \right) \psi_{3D}(x',y',z';t') = 0. \quad (A4)$$

Demonstration. By use of Eqs. (A2), (A3) and of assumption (A1), one obtains, by direct calculations, that

$$\left(\partial_{x'}^2 + \partial_{y'}^2 + \partial_{z'}^2 - \frac{1}{c^2} \partial_{t'}^2 \right) \psi_{3D}(x',y',z';t')$$

$$= \left(\sin^2 \theta \, \partial_x^2 + \sin^2 \theta \, \partial_y^2 + \frac{\cos^2 \theta}{c^2} \partial_t^2 - \frac{1}{c^2} \partial_t^2 \right) \psi_{2D}(x,y;t)$$

$$= \sin^2 \theta \left(\partial_x^2 + \partial_y^2 - \frac{1}{c^2} \partial_t^2 \right) \psi_{2D}(x,y;t) = 0,$$

so that the theorem gets demonstrated.

[1] M. Zamboni Rached, E. Recami, and F. Fontana, Phys. Rev. E **64**, 066603 (2001).

[2] H. Bateman, *Electrical and Optical Wave Motion* (Cambridge University Press, Cambridge, 1915); see also, J. A. Stratton, *Electromagnetic Theory* (McGraw-Hill, New York, 1941), p. 356.

[3] A. O. Barut *et al.*, Phys. Lett. A **143**, 349 (1990); Found. Phys. Lett. **3**, 303 (1990); Found. Phys. **22**, 1267 (1992).

[4] A. O. Barut *et al.*, Phys. Lett. A **180**, 5 (1993); **189**, 277 (1994).

[5] R. Donnelly and R. W. Ziolkowski, Proc. R. Soc. London A **440**, 541 (1993); I. M. Besieris, A. M. Shaarawi, and R. W. Ziolkowski, J. Math. Phys. **30**, 1254 (1989); S. Esposito, Phys. Lett. A **225**, 203 (1997); J. Vaz and W. A. Rodrigues, Adv. Appl. Cliff. Alg. **S-7**, 457 (1997).

[6] R. Courant and D. Hilbert, *Methods of Mathematical Physics* (Wiley, New York, 1966), Vol. 2, p. 760; cf. also, J. N. Brittingham, J. Appl. Phys. **54**, 1179 (1983); R. W. Ziolkowski, J. Math. Phys. **26**, 861 (1985); J. Durnin, J.J. Miceli, and J.H. Eberly, Phys. Rev. Lett. **58**, 1499 (1987); A. M. Shaarawi, I. M. Besieris, and R. W. Ziolkowski, J. Math. Phys. **31**, 2511 (1990); P. Hillion, Acta Applicandae Matematicae **30**, 35 (1993).

[7] A. O. Barut, G. D. Maccarrone, and E. Recami, Nuovo Cimento A **71**, 509 (1982); E. Recami *et al.*, Lett. Nuovo Cimento **28**, 151 (1980); *ibid.* **29**, 241 (1980).

[8] E. Recami, Riv. Nuovo Cimento **9**(6), 1 (1986); cf. also E. Recami, F. Fontana, and R. Garavaglia, Int. J. Mod. Phys. A **15**, 2793 (2000); E. Recami *et al.*, Il Nuovo Saggiatore **2**(3), 20 (1986); **17**(1-2), 21 (2001); Found. Phys. **31**, 1119 (2001).

[9] J.-y. Lu and J. F. Greenleaf, IEEE Trans. Ultrason. Ferroelectr. Freq. Control **39**, 19 (1992).

[10] R. W. Ziolkowski, I. M. Besieris, and A. M. Shaarawi, J. Opt. Soc. Am. A **10**, 75 (1993).

[11] E. Recami, Physica A **252**, 586 (1998); see also J.-y. Lu, J. F. Greenleaf, and E. Recami, e-print physics/9610012; cf. also E. Recami, in *Time's Arrows, Quantum Measurement and Superluminal Behavior*, edited by D. Mugnai, A. Ranfagni, and L. S. Shulman (C.N.R., Rome, 2001), pp. 17–36.

[12] M. Zamboni Rached, E. Recami, and H. E. Hernández-Figueroa, e-print physics/0109062; Europ. Phys. J. D. **21**, 217 (2002).

[13] J.-Y. Lu and J. F. Greenleaf, IEEE Trans. Ultrason. Ferroelectr. Freq. Control **39**, 441 (1992) [in this case the beam speed is larger than the *sound* speed in the considered medium].

[14] P. Saari and K. Reivelt, Phys. Rev. Lett. **79**, 4135 (1997).

[15] D. Mugnai, A. Ranfagni, and R. Ruggeri, Phys. Rev. Lett. **84**, 4830 (2000); [For a panoramic review of the ''superluminal'' experiments, see E. Recami, Found. Phys. **31**, 1119 (2001); e-print physics/0101108].

[16] Cf. also, e.g., A. M. Shaarawi and I. M. Besieris, J. Phys. A **33**, 7227 (2000); **33**, 7255 (2000); **33**, 8559 (2000); Phys. Rev. E **62**, 7415 (2000).

[17] See, e.g., R.E. Collin, *Field Theory of Guided Waves* (IEEE Press, New York, 1991).

[18] J.-Y. Lu, H.-H. Zou, and J. F. Greenleaf, IEEE Trans. Ultrason. Ferroelectr. Freq. Control **42**, 850 (1995).

[19] See, e.g., E. Butkov, *Mathematical Physics* (Addison-Wesley, Reading, MA, 1968).

[20] See, e.g., J. D. Jackson, *Classical Electrodynamics* (J. Wiley, New York, 1975).

[21] Cf., e.g., S. Ramo, J. R. Whinnery, and T. Van Duzer, *Fields and Waves in Communication Electronics* (John Wiley, New York, 1984), Chap. 8.

[22] Cf., e.g., the first one of Ref. [11], and references therein.

[23] See, e.g., M. Zamboni Rached and H. E. Hernández-Figueroa, Opt. Commun. **191**, 49 (2000). From the experimental point of view, cf., e.g., S. Longhi, P. Laporta, M. Belmonte, and E. Recami, Phys. Rev. E **65**, 046610 (2002); cf. also V. S. Olkhovsky, E. Recami, and G. Salesi, Europhys. Lett. **57**, 879 (2002); Y. Aharonov, N. Erez, and B. Reznik, Phys. Rev. A **65**, 052124 (2002).

[24] I. M. Besieris, M. Abdel-Rahman, A. Shaarawi, and A. Chatzipetros, Prog. Electromagn. Res. (PIER) **19**, 1 (1998).